Urban Water Journal
Publication details, including instructions for authors and subscription information:
http://www.tandfonline.com/loi/nurw20

The combined use of resilience and loop diameter uniformity as a good indirect measure of network reliability

Enrico Creaco[a], Marco Franchini[b] & Ezio Todini[c]
[a] College of Engineering, Mathematics and Physical Sciences, University of Exeter, Exeter, UK
[b] Department of Engineering, University of Ferrara, Ferrara, Italy
[c] BiGeA University of Bologna, Bologna, Italy
Published online: 12 Sep 2014.

To cite this article: Enrico Creaco, Marco Franchini & Ezio Todini (2014): The combined use of resilience and loop diameter uniformity as a good indirect measure of network reliability, Urban Water Journal

To link to this article: http://dx.doi.org/10.1080/1573062X.2014.949799

Urban Water Journal, 2014
http://dx.doi.org/10.1080/1573062X.2014.949799

Taylor & Francis
Taylor & Francis Group

RESEARCH ARTICLE

The combined use of resilience and loop diameter uniformity as a good indirect measure of network reliability

Enrico Creaco[a]*, Marco Franchini[b] and Ezio Todini[c]

[a]*College of Engineering, Mathematics and Physical Sciences, University of Exeter, Exeter, UK;* [b]*Department of Engineering, University of Ferrara, Ferrara, Italy;* [c]*BiGeA University of Bologna, Bologna, Italy*

(*Received 28 November 2013; accepted 23 June 2014*)

The aim of this paper is to show that the combined use of the resilience index (Todini, 2000) with a loop based diameter uniformity index (here formulated) yields a good indirect reliability measure, which can be conveniently used within the optimization processes of the water distribution system design. The methodology adopted to show the advantages of the combined use of the two indexes consists of (a) a three-objective optimization performed in order to simultaneously minimize costs (first objective function) and maximize both the resilience and the loop diameter uniformity indexes (second and third objective functions respectively); (b) a retrospective assessment of performance indicators relative to critical operational scenarios on the solutions of the Pareto surface obtained at the end of the optimization process. Applications were performed considering a simple case study, which made it possible to easily compare the new approach, based on a three-objective optimization, with the two-objective optimization process based on the use of the resilience index alone and also with the two-objective optimization process based on the modified resilience index formulated by Prasad, Sung-Hoon, and Namsik (2003) (where the diameter uniformity is defined at nodal level and inserted as a weight in Todini's resilience index), being both indexes a surrogate to reliability. The comparison pointed out that using resilience and loop diameter uniformity as two separate objective functions in an optimization process leads to solutions which perform better during critical operational scenarios (particularly when dealing with segment isolation) than the equally expensive solutions obtained adopting the resilience index (independently of its formulation) alone as reliability related objective function. Since the proposed approach suggests that a three-objective optimization be utilized to perform an appropriate pipe-network optimal design, an improvement in the well-known NSGA-II algorithm (Deb, Pratap, Agarwal, & Meyarivan, 2002) is proposed as its original formulation proved to have some difficulties dealing with more than two objectives.

Keywords: resilience; loop; diameter uniformity; water distribution modeling; design; optimization

Introduction

The reliability of a water system was originally defined by Hashimoto, Loucks, and Stedinger (1982) as the probability that the system operation does not fail within a pre-selected time interval. Later, in the context of water distribution systems, the concept of reliability has more and more often been flanked by the concept of performance, which can be evaluated by means of suitable indicators (Gargano & Pianese, 2000; Tanyimboh, Tabesh, & Burrows, 2001; Ciaponi, 2009; Creaco & Franchini, 2012). These performance indicators usually express the ratio of water discharge supplied to users to the corresponding water demand and can be evaluated under various operational scenarios, including normal peak operating conditions and critical operational scenarios such as those related to mechanical (pipe breakage, pump failure, power outages, control valve failure, etc.) and hydraulic (such as changes in demand or in pressure head, ageing of pipes, inadequate pipe sizing, insufficient pumping capacity, insufficient storage capability) failures (Mays, 1996). By evaluating the performance indicators under various scenarios and calculating the weighted mean on the basis of weights related to the scenario occurrence probabilities, a measure of the reliability can then be derived (Ciaponi, 2009). Though enabling an accurate estimation of reliability, performance indicators have the drawback of requiring numerous *pressure-driven* hydraulic simulations for their assessment; the computational burden associated with their use in the optimization context (for the design or rehabilitation of water distribution networks) may then turn out to be prohibitive.

In order to have an expeditious reliability estimation, which can be fruitfully utilized in the optimization context also when real complex systems are considered, indirect compact indexes (Gessler & Walski, 1985; Todini, 2000; Prasad, Sung-Hoon, & Namsik, 2003; Farmani, Savic, & Walters, 2003; Farmani, Walters, & Savic, 2005, 2006; Prasad & Park, 2004; Raad, Sinske, & van Vuuren, 2010a, 2010b; Creaco & Franchini, 2012, 2014a; Wang, Savic, & Kapelan, 2014) can be considered, which do not require a

*Corresponding author. Email: E.F.Creaco@exeter.ac.uk

statistical/probabilistic analysis of the network performance under various operational scenarios. As a matter of fact, they can be evaluated by means of a single (also demand-driven) hydraulic simulation, in a bid to express the network redundancy under benchmark operating conditions. This network redundancy is a reserve which can be exploited to overcome possible failures under critical operational scenarios. In detail, during multi-objective optimizations aimed at obtaining trade-off solutions between cost and reliability, an indirect compact index can be considered as an objective function surrogate to reliability to be maximized while the objective function cost is being minimized.

Among these indexes, there exist two main categories: pressure head/energy related indexes (Gessler & Walski, 1985; Todini, 2000; Prasad et al., 2003) and flow paths-related indexes (Tanyimboh & Templeman, 2000; Tanyimboh, Tietavainen, & Saleh, 2011). Most works aimed at comparing the two categories of indexes (Raad et al., 2010a; Greco, Di Nardo, & Santonastaso, 2012; Creaco, Fortunato, Franchini, & Mazzola, 2014) pointed out a higher correlation between the pressure head/energy based indexes and reliability than between flow paths-related indexes and reliability.

Among the pressure head/energy related indexes, the first index proposed was the surplus index *IS* (Gessler & Walski, 1985), which relates to the minimum head surplus at a node which is considered as the critical one in the network and can be calculated through the following formula:

$$IS = \min_{i=1,\dots,n_n} (h_i - h_{des,i}) \tag{1}$$

where h_i is the piezometric height at the generic i-th of the n_n demanding nodes and $h_{des,i}$ is the minimum desired piezometric height value which guarantees full demand satisfaction at the same node.

The surplus index has the drawbacks of being related to a single node of the network (and thus is not able to yield indications of the whole head surplus condition), of not being in dimensionless form and of not giving any information on the level of discharge delivered at the node where *IS* is computed. With these shortcomings in mind, Todini (2000) proposed the resilience index, which is related to the whole network, i.e. to all the n_n demanding nodes, and takes on the following dimensionless form, expressing the ratio of the power excess supplied to the users to the power excess leaving the sources:

$$I_r = \frac{\sum_{i=1}^{n_n} q_{dem,i}(h_i - h_{des,i})}{\sum_{k=1}^{n_r} Q_k H_k - \sum_{i=1}^{n_n} q_{dem,i} H_{des,i}} \tag{2}$$

where $q_{dem,i}$ is the demand of the i-th network node and Q_k and H_k are the water discharge leaving the generic k-th of the n_r source points and the relative head respectively. Finally, $H_{des,i} = h_{des,i} + z_i$, with z_i being the nodal elevation. Another advantage of the resilience index with respect to the surplus index lies in the fact that in Equation (2) the piezometric height surplus of the generic node is weighted by means of the demand of the node itself; thus, the excess at nodes featuring higher demand values yields a larger contribution in terms of the network resilience. In the design phase, since $h_i \geq h_{des,i}$, the resilience index generally ranges from 0 to 1, the lower and higher values corresponding to networks with small and large diameter pipes respectively.

Later, various authors (Prasad et al., 2003; Raad et al., 2010a; Pandit & Crittenden, 2012) proposed modified versions of Todini's resilience. Among all the modified resilience formulas, that proposed by Prasad et al. (2003) is that which has lately been more widely used (Prasad and Park, 2004; Raad et al., 2010b; Creaco and Franchini, 2014a; Wang et al., 2014). In detail, in order to take account of the fact that the uniformity of pipes helps the network keeping high reliability service during segment isolations, Prasad et al. (2003) included a diameter uniformity coefficient in the resilience formula, which was then written as:

$$I_{r,mod} = \frac{\sum_{i=1}^{n_n} C_i q_{dem,i}(h_i - h_{des,i})}{\sum_{k=1}^{n_r} Q_k H_k - \sum_{i=1}^{n_n} q_{dem,i} H_{des,i}} \tag{3}$$

where the diameter uniformity coefficient C_i expresses the ratio of the mean to the maximum diameter of the pipes connected to the generic i-th of the n_n demanding nodes.

Though Creaco, Fortunato, Franchini, & Mazzola, (2014) showed that the modified resilience (Equation (3)) represents the network performance during segment isolation better than the original resilience (Equation (2)), a drawback of Equation (3) lies in the fact that the presence of the empirical coefficient C in the numerator of Equation (3) causes the formula to lose its original physical meaning, essentially based on a ratio of powers. Furthermore, it is generally agreed that the network performance is more related to the uniformity of the pipe diameters in the generic loop, rather than to the uniformity of the diameters of the pipe connected to the generic node, as is assumed in the form of Equation (3). Indeed, the loop diameter uniformity represents a complementary ingredient to resilience for network reliability.

In the present work, the writers aim at proving that considering the network resilience I_r and the loop diameter uniformity (defined in the next section) as two distinct objectives to be simultaneously maximized during an optimization process while minimizing the cost, leads to a better compromise representation of the network reliability than that obtained by trading-off the minimization of the costs with the maximization of the resilience I_r or of the modified $I_{r,mod}$ resilience alone.

The remainder of the paper is organized as follows. The next section concerns the methodology adopted, where firstly the loop diameter uniformity is defined and then the optimization framework is described. The application section, which describes the case studies considered and then reports the analysis of the results, and the conclusions follow.

An additional innovative contribution of the paper is also that presented in the Appendix where a modified NSGA-II (Deb, Pratap, Agarwal, & Meyarivan, 2002) multi-objective optimization algorithm is formulated in order to make it more efficient when dealing with more than two objective functions.

Methodology

As explained above, loop diameter uniformity is an aspect which ought to be considered as an objective function independent of resilience within optimization processes. To this end, we introduce the following loop diameter uniformity coefficient, obtained as a function of the average of the diameter uniformity C_l in each loop through the following formula:

$$C_u = \frac{n_{pwithloop}}{n_p} \frac{\sum_{l=1}^{nl} C_l}{n_l} \quad (4)$$

where $n_{pwithloop}$ is the number of pipes which belong to (at least) one loop (and thus all the pipes only belonging to branched structures are not included in $n_{pwithloop}$) and n_p is the total number of pipes in the network; C_l is calculated as the ratio of the mean to the maximum diameter of the generic l-th of the n_l loops. From a general point of view, C_u varies from solution to solution during an optimization process because:

- $n_{pwithloop}$ can increase when pipes are added in parallel at certain pipe sites;
- C_l changes when the diameters of the pipes which belong to a certain loop change.

In order to show that considering the coefficient in Equation (4) as an independent objective function leads to a better representation of reliability, a two-step methodology is herein considered.

In Step 1, multi-objective design optimizations, aimed at simultaneously minimizing network total cost and maximizing the reliability, expressed in terms of one or two indirect indexes, are performed on a water distribution network considering, as decisional variables, the network pipe diameters. The results of the optimizations are Pareto fronts (or surfaces) of optimal solutions featuring increasing values of the network cost and of the indirect indexes.

In Step 2, in order to understand which of the reliability indirect indexes yields the best representation of the network reliability as the cost grows, for each of the optimization performed, all the optimal solutions of the Pareto front/surface are *a posteriori* assessed in terms of direct performance indicators relative to the critical operational scenarios of network segment isolation and hydrant service, as proposed in Creaco and Franchini (2012). This retrospective assessment makes it possible to obtain relationships between the latter direct performance indicators and the costs produced by the different optimizations. Results are then compared and the best optimization approach, which leads to the highest (direct) reliability levels for given cost, is detected. In other words, the best optimization approach will give an indication of the best indirect measure of reliability in the framework of network design.

At this stage, a remark has to be made about the fact that the whole work was developed under the assumption that the network design is performed in a single step, without considering the real gradual growth of the nodal demands and of the network layout in time. In actual fact, recent studies (Basupi & Kapelan, 2013; Creaco, Franchini, & Walski, 2014a, 2014b) have shown that, rather than a single step design, a multi-step design should be performed in order to follow the network growth. The single step design was used herein with the objective to simplify the analysis of the results, which is only aimed at investigating the effects of the choice of a compact reliability index within the optimization context.

In the two following sub-sections, the description of the various optimizations carried out and of the performance indicators adopted is reported.

Optimizations with indirect reliability indexes as objective functions

Three different optimizations (optimizations I, II and III) are performed using the version of the NSGA-II multi-objective algorithm (Deb et al. 2002) proposed by Creaco, Franchini, and Alvisi (2010) and then later also used by Alvisi, Creaco, and Franchini (2011), in which individual genes can take on integer values.

Whereas the total cost of the installed pipes is the first objective function to be minimized in all the optimizations, the optimizations differ in the index or indexes adopted as indirect measure of reliability to be maximized within the optimization process:

Optimization I – one reliability related objective, the resilience index I_r by Todini (2000), Equation (2);
Optimization II – one reliability related objective, the modified resilience index $I_{r,mod}$ by Prasad et al. (2003), Equation (3);
Optimization III – two reliability related objectives, the resilience index I_r by Todini (2000), Equation (2),

and the coefficient C_u of loop diameter uniformity, Equation (4).

For the application of Equation (4), the (minimum) loops of the network have to be detected. To this end the procedure proposed by Creaco and Franchini (2014b), also suitable for topologically complex networks, can be conveniently used.

In each optimization, a demand-driven hydraulic simulation was performed using the Global Gradient Algorithm of Todini and Pilati (1988) in order to calculate network nodal pressure heads and, subsequently, the resilience indexes. The use of the demand driven approach is justified by the fact that in the design phase a standard operational scenario is considered, where all the network nodes have to lie above the pressure head value required for full demand satisfaction. Network configurations which feature some nodal pressure heads lower than the desired value are penalized during the optimization.

It is worth underlining that for optimization III (with three objectives), the NSGA II algorithm was further modified in order to obtain a sufficiently spread Pareto surface without the necessity to increase the number of individuals and generations (see the Appendix for more details) thereby making it more efficient in dealing with three objective functions.

Performance indicators

Following the optimization step, the optimal solutions obtained can be retrospectively assessed under critical operational scenarios, in which pressure heads can be lower than the desired threshold at some network nodes. In order to represent pressure-dependent outflows when nodal pressure heads are different from the desired value, the pressure driven approach was adopted. To this end an upgraded version of the Global Gradient Algorithm of Todini and Pilati (1988) was used (see, for instance, Alvisi & Franchini, 2006).

As a performance indicator, direct measure of reliability, for a given operational scenario j, the demand satisfaction rate S_j, defined as follows (Creaco & Franchini, 2012), can be adopted:

$$S_j = \frac{\sum_{i=1}^{n_n} q_i}{\sum_{i=1}^{n_n} q_{dem,i}} \tag{5}$$

where q_i is the actual water flow supplied to users at the i-th node, calculated on the basis of a *pressure-driven* simulation of the network under the j-th scenario. The relationship between water discharge q_i and water demand $q_{dem,i}$ depends on the value of the nodal piezometric height and can be expressed as follows (Wagner, Shamir, & Marks, 1988):

$$\begin{cases} q_i = 0 & h_i \le h_{min,i} \\ q_i = q_{dem,i}\left(\frac{h_i - h_{min,i}}{h_{des,i} - h_{min,i}}\right)^{\delta} & \text{for} \quad h_{min,i} \le h_i \le h_{des,i} \\ q_i = q_{dem,i} & h_i \ge h_{des,i} \end{cases} \tag{6}$$

where $h_{min,i}$ is the minimum pressure head required to enable nodal outflow; the exponent δ is commonly set at 0.5 (see Aoki, 1998).

Among the various possible operational scenarios, those featuring service disruption in some parts of the network (segments), which can be isolated from the water sources by operating isolation valves, are particularly relevant. S_j can be assessed with reference to operational scenarios in which a single segment is isolated at a time. Assuming that the network can be subdivided into n_s independent segments, it is possible to evaluate the S_j index associated with the operational scenario corresponding to the isolation of the generic network segment j, by performing a pressure driven hydraulic simulation for the part of the network remaining connected to the water sources after the isolation of the segment itself. After assessing S_j for the generic segment, the performance indicator "average satisfaction" I_{aS} (aS: average-Satisfaction) of the whole network can be calculated by averaging the demand satisfaction rate relative to each segment isolation as follows:

$$I_{aS} = \frac{\sum_{j=1}^{n_s} S_j}{n_s} \tag{7}$$

It is worth underlining that in Equation (7) all the segment isolation scenarios are equally weighted. This means that, for the sake of simplicity, the same failure probability is implicitly assigned to all such scenarios. Should this simplifying assumption not be acceptable under specific circumstances, Equation (7) could be upgraded in order to account for different failure probabilities for the various network segments.

Further possible critical scenarios are those featuring the activation of a hydrant at a generic node. Assuming the presence of a hydrant at n_{nh} of the network nodes, the performance indicator "average satisfaction during fire conditions" I_{afS} (afS: average-fire-Satisfaction) can be assessed as:

$$I_{afS} = \frac{\sum_{j=1}^{n_{nh}} S_j}{n_{nh}} = \frac{1}{n_{nh}} \sum_{j=1}^{n_{nh}} \frac{\sum_{i=1}^{n_n} q_{i,j}}{\sum_{i=1}^{n_n} q_{dem,i}} \tag{8}$$

where $q_{i,j}$ is the actual discharge delivered at node i when the j-th hydrant is activated. It has to be noted that the formula in Equation (8) for assessing performance indicator I_{afS} gives the same weight to the hydrant activations at the various network nodes. This means that Equation (8) entails the simplifying assumption of uniform probability of fire in the various parts of the network.

Under specific conditions, Equation (8) could then be improved to account for not uniform fire probability.

To describe network performance as regards the operation of a hydrant at the generic j-th node, the following $S_{h,j}$ index can be introduced:

$$S_{h,j} = \frac{q_{hydr,j}}{d_{hydr}} \tag{9}$$

in which d_{hydr} and $q_{hydr,j}$ are the required and actual hydrant discharges, respectively (it is implicitly assumed that d_{hydr} is the same for all the hydrants). The relationship between $q_{hydr,j}$ and d_{hydr} takes on the following form:

$$q_{hydr,j} = d_{hydr}\left(\frac{h_j}{h_{\text{jmin}}}\right)^{0.5} \tag{10}$$

which yields $q_{hydr,j} = d_{hydr}$ when $h_j = h_{jmin}$. Setting the exponent at 0.5 in Equation (10) is due to the fact that the hydrant behaves like a pressurized orifice (Walski et al., 2003). Should h_j be larger (smaller) than h_{jmin} at the generic node, $q_{hydr,j}$ would be larger (smaller) than the required outflow value d_{hydr}.

A global performance indicator "average satisfaction of hydrants" I_{ah} (ah: average-hydrant) can also be evaluated with reference to the total number n_{nh} of hydrants installed:

$$I_{ah} = \frac{\sum_{j=1}^{n_{nh}} S_{h,j}}{n_{nh}} \tag{11}$$

Like in Equation (7) as to the segment isolation scenarios, all the hydrant activation scenarios are equally weighted in Equation (8) and Equation (11) since the hydrant activation probability is assumed to be uniform over the network nodes. Like Equations (7) and (8), Equation (11) could also be upgraded in order to take more general conditions into consideration.

Application

Case-study

The case study considered herein is the network (Figure 1), made up of $n_n = 23$ nodes with outflow, all with ground elevation of 0 m, and 29 pipe sites, where the term "pipe

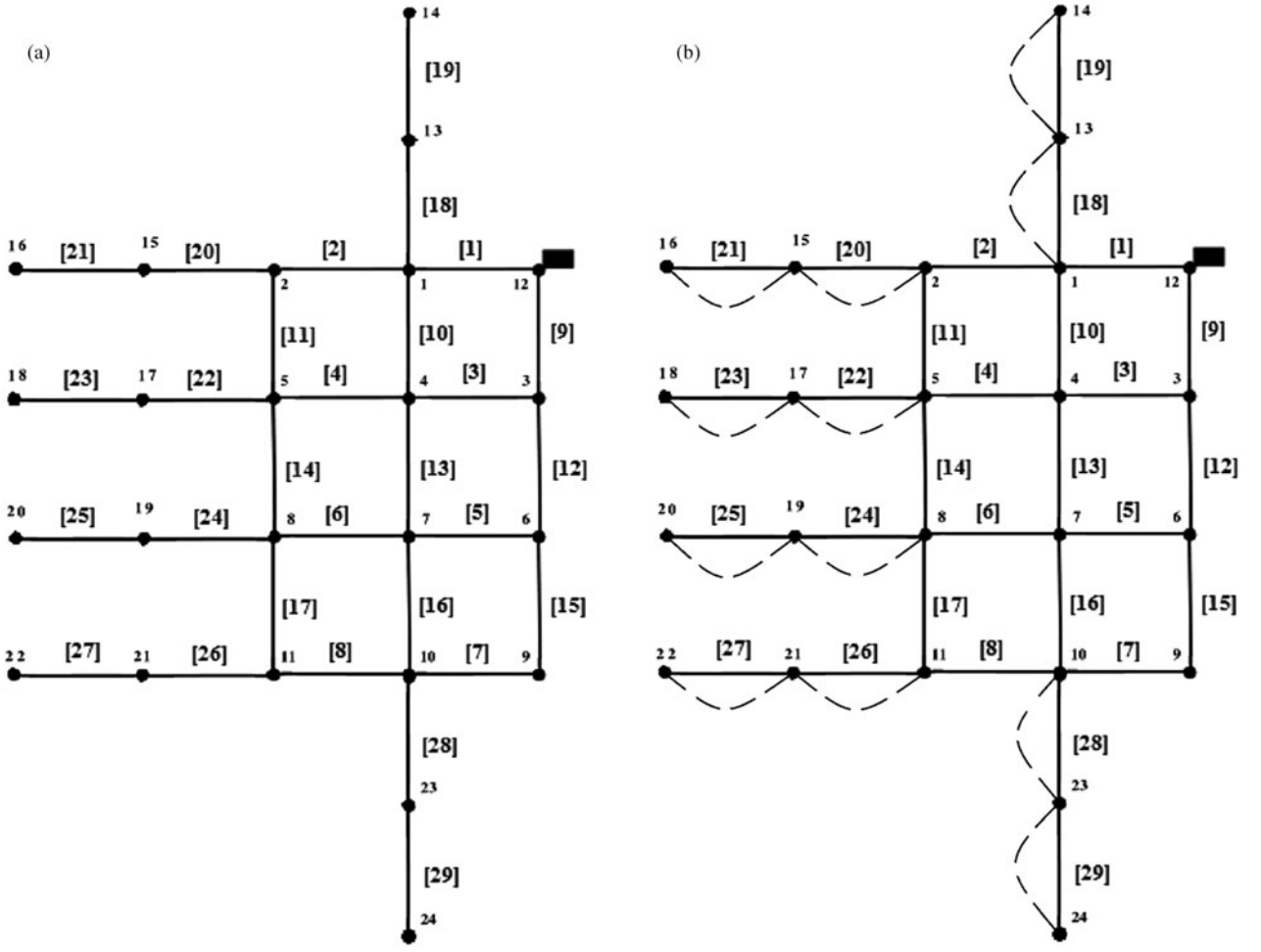

Figure 1. Layouts a and b of the network considered for the applications. Pipe site numbers inside the brackets []. Dotted lines in layout b indicate the pipes which can be installed in parallel.

site" indicates a place where a single pipe or more pipes in parallel can be laid. In every pipe site, a length equal to 1000 m and a Hazen-Williams roughness coefficient equal to 130 were considered for each pipe laid. The network features a global peak demand of 444.5 l/s. The q_{dem} values for each node are reported in the following Table 1. The choice of such a simple network for the applications is motivated by the necessity of facilitating the analysis of the results and the comparison between the different approaches. Furthermore, when the network features a very simple topology, optimization algorithms are more efficient. Should more complicated networks be used, other issues (such as the capability of the generic optimization algorithm to get really close to the real optima) could make the investigation more complicated and distorted by other aspects, thus obscuring the main objective of the current research.

The head of the only reservoir present in the network at node 12 is set at 50 m. The minimum desired pressure for full demand satisfaction is $h_{des,i} = h_{des} = 30$ m in all the nodes.

Overall, two sets of optimizations were performed: in set A, only one pipe was considered to be installable at each pipe site of the network; this entails that a total number of loops $n_l = 6$ is always considered in set A for layout a) in Figure 1a, since pipes 18–29 are always branched structures. Set B differs from set A in that at pipe sites 18–29 up to two pipes can be installed in parallel (thus forming a loop between two consecutive nodes), as is shown in Figure 1b; a total number of loops ranging from 6 to 18 is then derived for set B, the highest value obtained when at all pipe sites 18–29 two pipes are installed. Allowing for the installation of two parallel pipes at each of pipe sites 18–29 complies with the commonly adopted design practice to avoid the presence of branched structures when high performance of supply to users has to be guaranteed in the network under all operating conditions, above all in segment isolation scenarios.

In each optimization of either set, a population of 200 individuals and a total number of generations equal to 2000 were considered, since a preliminary analysis had showed that these values allow a good tradeoff between computation times and accuracy of the results.

In each population individual, a number of genes equal to the pipes which can be installed in the layout in Figure 1 is considered, i.e. 29 in set A and 41 in set B. As to set B, pipes 30–41 are the pipes which can be laid in parallel to pipes 18–29 at pipe sites 18–29. Individual genes from 1 to 29 are assumed to take on values within the range 1-n_D, with n_D being the total number of pipe diameters considered for the design, in order to indicate the diameter ID. In optimization set B, individual genes 30–41 are assumed to take on values within the range 0-n_D, where the 0 value helps considering the not installed pipe condition.

In all the optimizations, two preset individuals were considered in the initial population, the first corresponding to a minimum cost solution and the second obtained by considering the maximum diameter (600 mm) for all the network pipes (maximum cost solution).

The values of the unit pipe cost for the $n_D = 12$ diameters considered in the applications are reported in the following Table 2.

For the post-processing of solutions and the assessment of performance indicators, the exponent δ of Equation (6) was set at 0.5 (Aoki, 1998) whereas the lowest pressure head value $h_{min,i} = h_{min}$ that ensures nodal outflow was fixed at 5 m in all the nodes. The values of δ and h_{min}

Table 1. Characteristics of the demanding nodes in terms of demand.

Node ID	Demand q_{dem} (L/s)
1	13.48
2	20.22
3	20.22
4	20.22
5	13.48
6	26.91
7	26.91
8	26.91
9	13.48
10	20.22
11	13.48
13	13.48
14	20.22
15	20.22
16	20.22
17	13.48
18	26.91
19	26.91
20	26.91
21	13.48
22	20.22
23	13.48
24	13.48

Table 2. Pipe diameters, D, and unit costs, c, adopted during the design phase.

Diameter ID	D[mm]	c [€/m]
1	45	185
2	60	203
3	80	227
4	100	231
5	150	272
6	200	299
7	250	328
8	300	360
9	350	399
10	400	439
11	500	503
12	600	581

considered in this paper are in agreement with those used by previous authors, such as Gargano and Pianese (2000), Tanyimboh et al. (2001) and Creaco and Franchini (2012).

For the formation of segments, isolation valves are generally positioned according to the *N*-1 or *N* valve rules. As was described by Walski, Weiler, and Culver (2006), these rules consist in applying, in proximity to each node, valves in all or all but one the linked pipes respectively. In this work, the *N* valve rule was considered, entailing that isolation valves are placed at either end node of each pipe. Each pipe was then considered as an independent segment.

Hydrants were assumed to be installed at all network demanding nodes. For hydrant operation, a value of $h_{jmin} = 30$ m was assumed in Equation (10).

The optimizations were run on a single processor of a 2.70 GHz DualCore unit in the Matlab®2011b environment.

In the following section, the results of either optimization set are reported.

Results

Optimization set A

The duration of optimizations I (with resilience index I_r as objective function) and II (with modified resilience index $I_{r,mod}$ as objective function) was about 20 min, whereas the duration of optimization III (with resilience index I_r and loop diameter uniformity as separate objective functions) was about 30 min. The reasons for the slight increase in the computation time in the case of optimization III are described in the Appendix.

The results in terms of Pareto front relative to set A optimizations I, II and III are reported in the following Figure 2. In this context, it has to be stressed that whereas the results of optimizations I and II are 2D Pareto fronts of trade off optimal solutions, the results of optimization III represent a 3D Pareto surface. However, in order to make the results of optimization III easier to read, they were plotted as dots on a 2D graph and the value of the third objective C_u was represented through the color of the dot (light color dots represent small values whereas dark dots represent large values). All the fronts comprise solutions ranging from about 9×10^6 € to about 17×10^6 € in terms of cost and from about 0.3 to about 0.95 in terms of resilience I_r (or modified resilience $I_{r,mod}$). As to optimization III, values of C_u within the range 0.27–0.59 were obtained, with the highest value being obtained for the solutions where the same size is proposed by the optimizer for pipes 1–17 (of course with increasing cost as the diameter increases), which belong to at least one loop; for these solutions, Equation (4) yields $C_u = n_{pwithloop}/n_p \approx 0.59$ since $\sum_{l=1}^{nl} C_l/n_l$ turns out to be equal to 1.

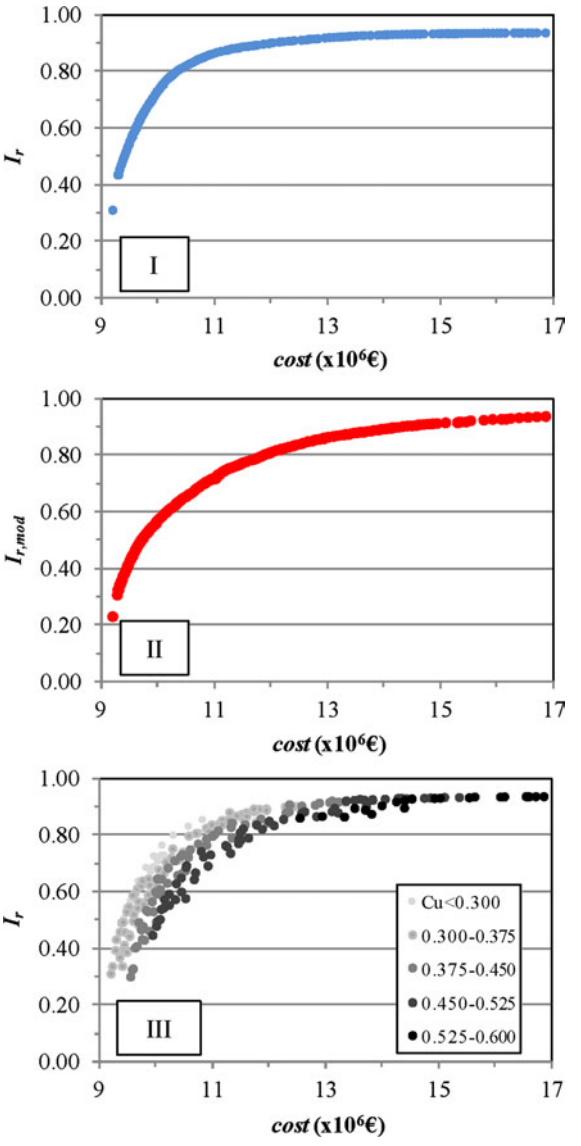

Figure 2. Set A. Pareto fronts of optimal solutions in the cost – resilience (or modified resilience) space obtained in the various optimizations. Optimal solutions corresponding to optimization I (min cost - max resilience I_r) are marked in blue, those corresponding to optimization II (min cost - max modified resilience $I_{r,mod}$) are marked in red and those corresponding to optimization III (min cost - max resilience I_r and loop diameter uniformity C_u) are marked in different tonalities of grey (light and dark grey corresponding to low and high C_u values respectively).

Each solution obtained in the three set A optimizations was retrospectively evaluated in terms of performance indicators I_{aS}, I_{afS} and I_{ah}. The graphs in Figure 3 report the relationship between each of the performance indicators and network cost. An aspect that comes out from Figure 3 is that, whereas, as was expected, I_{aS} and I_{afS} take on values which are always lower than or equal to 1, corresponding to the fact that the nodal outflows are always lower than or equal to the nodal demands (due to

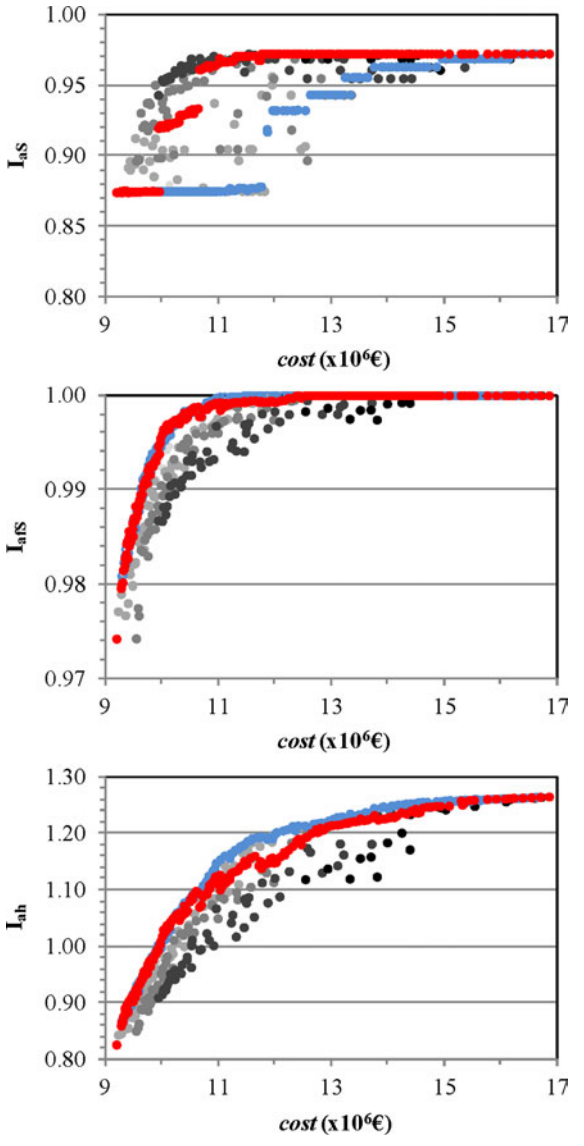

Figure 3. Set A. Direct performance indicators, I_{aS}, I_{afS} and I_{ah}, of the alternative network configurations yielded by the optimizations. Optimal solutions corresponding to optimization I (min cost - max resilience I_r) are marked in blue, those corresponding to optimization II (min cost - max modified resilience $I_{r,mod}$) are marked in red and those corresponding to optimization III (min cost - max resilience I_r and loop diameter uniformity C_u) are marked in different tonalities of grey (light and dark grey corresponding to low and high C_u values respectively).

the structure of Equation (6)), indicator I_{ah} takes on values larger than 1 for high cost solutions. This is due to the fact that, unlike Equation (6), Equation (10) does not put an upper limit to outflow $q_{hydr,j}$, which can also take on values larger than d_{hydr} at some hydrants. Then, in the cases of high network costs (i.e. when large diameters are installed), high nodal pressure heads (larger than h_{jmin}) may take place, entailing that $q_{hydr,j} > d_{hydr}$ (see Equation (10)) at various network nodes and thus leading to $I_{ah} > 1$.

In particular, Figure 3 makes it possible to compare the results of optimization I (resilience index I_r as objective function), optimization II (resilience index $I_{r,mod}$ modified by Prasad as objective function) and optimization III (resilience index I_r and diameter uniformity C_u as objective functions). The analysis of Figure 3 highlights that as to I_{afS} and I_{ah}, optimizations I and II yield very similar results. This means that, for prefixed value of cost, optimizations I and II yield network configurations which feature very close values of the performance indicators. The highest dots (for a given cost) of optimization III are also close to the results of optimizations I and II. The analysis of Figure 3 also shows that the highest dots of optimization III have light grey tonality, which means that the achievement of high values of performance indicators I_{afS} and I_{ah} (relative to hydrant activation and for given cost) does not require high values of diameter uniformity to take place.

As to I_{aS}, the results obtained by optimization I are dominated by those obtained by optimization II. As a matter of fact, for prefixed values of network cost, optimization II is able to yield network configurations which feature higher values of I_{aS}. Furthermore, the highest dots of optimization III, which are the dark dots corresponding to high value of C_u, dominate significantly the results of optimization I and II. This means that the achievement of high values of performance indicator I_{aS} (relative to segment isolation) requires high values of diameter uniformity to take place in the network, which can only be obtained thanks to the use of C_u as a separate objective function during the optimization process.

Summing up, the design based on optimization I (where the resilience I_r by Todini (2000) is used as indirect measure of reliability) produces solutions which perform well (i.e. they are reliable) in terms of fire conditions but poorly in terms of segment isolation; the design based on optimization III (where the resilience index I_r by Todini is used in combination with the index C_u representing the diameter uniformity at loop level) enables a better discrimination between different solutions: those which perform better in terms of segment isolation are those with higher value of C_u while for a better behavior in terms of fire conditions smaller values of C_u are sufficient (i.e. uniformity is not necessary since fire hydrants do not significantly alter the flow patterns). Optimization II (where the resilience index $I_{r,mod}$ is used as indirect measure of reliability) produces intermediate results between those produced by the previous mentioned optimizations. This is not surprising since the latter indirect reliability index is structured in such a way that a sort of merging of I_r and C_u is performed (even though C_u is applied at node level rather than at loop level).

Optimization set B

In set B optimizations, a computation time very close to set A was observed.

The results in terms of Pareto front relative to optimization set B are reported in the following Figure 4. Compared to the fronts of optimization set A, the set B fronts also include solutions featuring costs within the range 17×10^6–25×10^6 €. This is due to the fact that in optimization set B two pipes are allowed in parallel at pipe sites 18–29 and the laying of extra pipes leads to the increase in the costs up to 25×10^6 €. The value range of the resilience index I_r, and of the modified resilience $I_{r,mod}$, of the set B-optimizations is only slightly larger than that obtained in the various set A-optimizations. As to optimizations I (with resilience index I_r as objective function) and II (with modified resilience index $I_{r,mod}$ as objective function), the set B Pareto fronts are actually coincident with the homologous set A fronts up to costs as large as 17×10^6 €. The only difference lies in the presence of the solutions with costs ranging from 17×10^6 to 25×10^6 € in set B Pareto fronts. The proximity of the solutions up to 17×10^6 € is due to the fact that during the optimizations I and II of set B the option of installing the parallel pipes at pipe sites 18–29 is indeed "activated" only after the largest pipe diameters have been assigned to the other pipes. As a matter of fact, optimizations I and II tend not to close the branched structures and leave them as they are. As to optimization III (with resilience index I_r and loop diameter uniformity C_u as separate objective functions), instead, the set B Pareto front is very different from the set A Pareto front. In particular, the solutions of the set B Pareto front take on C_u values within the range 0.27–1. As a matter of fact, set B optimization III makes it possible to achieve a value of C_u up to 1 since the installation of all the extra pipes in parallel at pipe sites 18–29 leads to the formation of new loops with respect to the set A optimization. As an example, the solutions with all the parallel pipes installed then feature $n_{pwithloop}/n_p = 1$; furthermore if pipe diameters are such as to guarantee the maximum loop diameter uniformity, $\sum_{l=1}^{nl} C_l/n_l = 1$, Equation (4) yields $C_u = 1$. By analyzing the set B Pareto front of optimization III, we notice that solutions featuring high C_u values (and then with the parallel pipes installed) are also present for low values of the cost (definitely smaller than 17×10^6 €). This means that optimization III gives more preference to the installation of parallel pipes for the formation of loops in correspondence to the branched structures of the network than optimizations I and II.

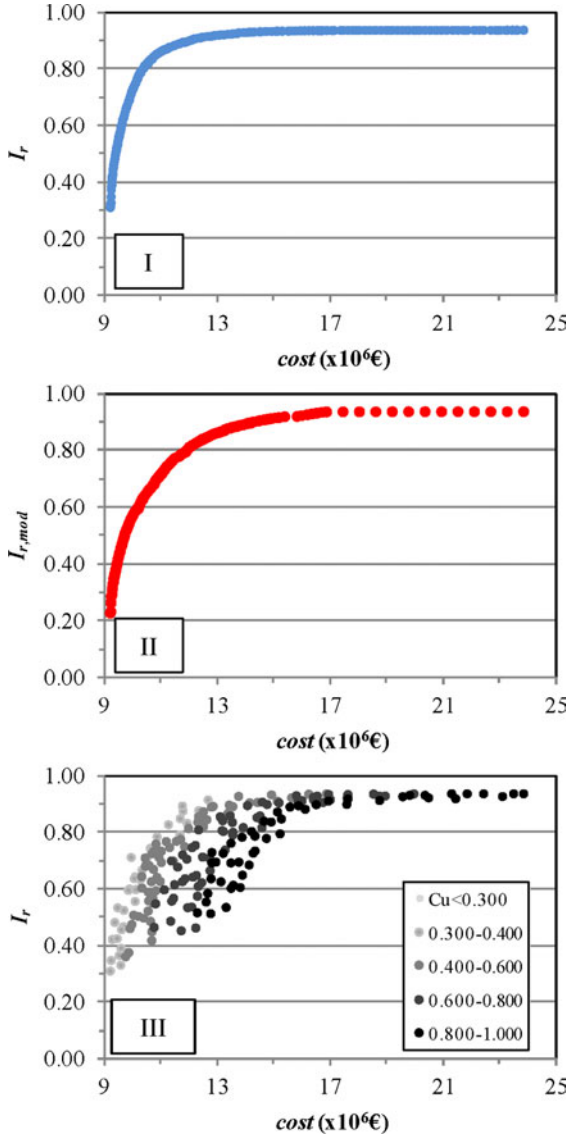

Figure 4. Set B. Pareto fronts of optimal solutions in the cost – resilience (or modified resilience) space obtained in the various optimizations. Optimal solutions corresponding to optimization I (min cost - max resilience I_r) are marked in blue, those corresponding to optimization II (min cost - max modified resilience $I_{r,mod}$) are marked in red and those corresponding to optimization III (min cost - max resilience I_r and loop diameter uniformity C_u) are marked in different tonalities of grey (light and dark grey corresponding to low and high C_u values respectively).

Each solution obtained in the three set B optimizations was retrospectively evaluated in terms of performance indicators I_{aS}, I_{afS} and I_{ah} and reported in the graphs in Figure 5.

Overall, the same remarks made as to I_{afS} and I_{ah} (indicators relative to fire conditions) for set A optimizations are still valid for set B optimizations. As to I_{aS} (relative to segment isolation), besides the confirmed superiority of optimization III, which is generally able to yield, for prefixed cost, more reliable solutions in terms of reliability than optimizations I and II, we may notice some new interesting aspects. First of all, unlike in Figure 3 relative to optimization set A, values of I_{aS} up to 1 are noticed in Figure 5 relative to optimization set B. This can be ascribed to the effects of the installation

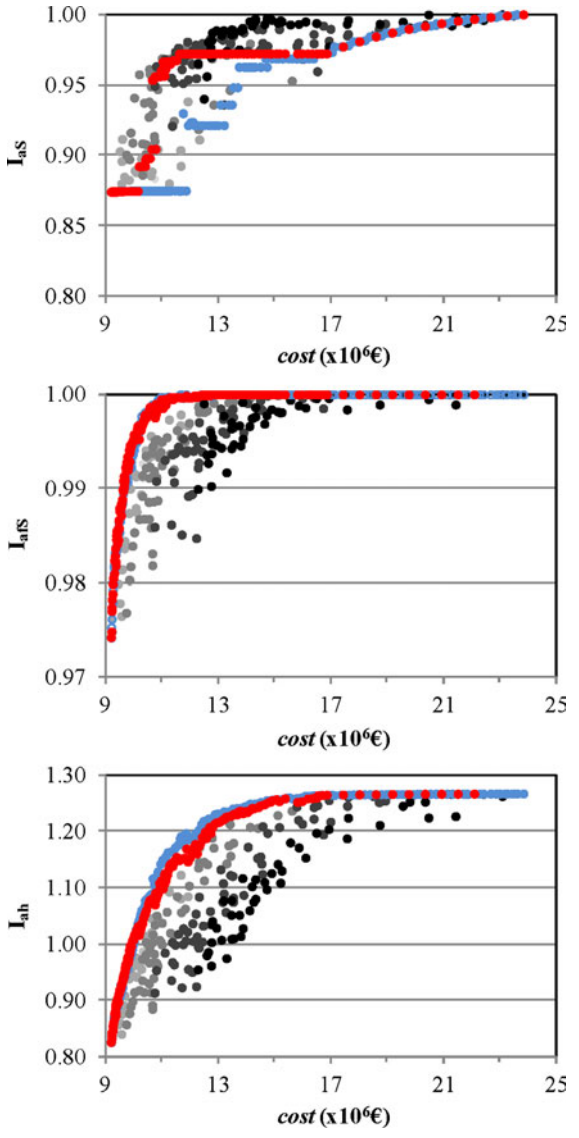

Figure 5. Set B. Direct performance indicators, I_{aS}, I_{afS} and I_{ah}, of the alternative network configurations yielded by the optimizations. Optimal solutions corresponding to optimization I (min cost - max resilience I_r) are marked in blue, those corresponding to optimization II (min cost - max modified resilience $I_{r,mod}$) are marked in red and those corresponding to optimization III (min cost - max resilience I_r and loop diameter uniformity C_u) are marked in different tonalities of grey (light and dark grey corresponding to low and high C_u values respectively).

of parallel pipes at sites 18–29 and to the subsequent formation of new loops, aspects which increase the network reliability significantly. However, whereas for the solutions of optimizations I and II the very high I_{aS} are obtained only for very high network cost, in the case of optimization III they are also obtained for more cost-effective solutions. This is due to the fact that optimization III encourages the installation of parallel pipes more than optimizations I and II and this may be ascribed to the fact that the two indexes I_r and C_u are kept separate.

As examples of diameter distribution in the network, four solutions (S1, S2, S3 and S4) were extracted from the Pareto front of optimization III in Figure 4. These four solutions, whose characteristics in terms of cost, resilience, loop diameter uniformity and performance indicators, are reported in Table 3, feature very close values of the cost and growing values of loop diameter uniformity. Figure 6 reports the diameter distribution of these solutions and points out that, whereas S1 and S2 feature the simultaneous presence of various large diameter (600 mm) and small diameter (45 mm) pipes close to each other, a higher diameter uniformity (around 400mm) is observed in solutions S3 and S4. Furthermore, whereas S1 and S2 feature no parallel pipe and only one parallel pipes respectively, numerous parallel pipes are present in S3 and S4 (8 and 7 respectively). The two aspects depicted above (higher diameter uniformity and presence of more numerous parallel pipes) connected with the growth of C_u have mainly a positive effect on the segments-related performance indicator I_{aS} which grows with C_u increasing. The effects on the fire conditions-related performance indicator I_{afS} and I_{ah}, instead, are negligible: whereas I_{afS} is almost constant, I_{ah} decreases while always assuming values larger than 1, which are acceptable. In the end, if a choice should be made among solutions S1–S4, either S3 or S4 should be preferred. Whereas all the four solutions are satisfactory as to fire conditions-related performance indicators, S3 and S4 show a better performance in terms of I_{aS}.

Final remarks

Both the conceptual viewpoint and the analysis of the results seem to point out that keeping the resilience index I_r separated from the diameter uniformity index C_u (at loop level) during the optimization process leads to the best results in the retrospective re-evaluation. The two variables represent different and complementary factors which affect the reliability. As a matter of fact, keeping them separated enables creation of a wider range of solutions where it is possible to identify those which perform better in terms of segment isolation and those which perform better in terms of fire conditions. Furthermore, it has the

Table 3. For solutions S1–S4 selected in the "Results" section and reported in Figure 6, values of cost, resilience I_r, loop uniformity C_u, and of performance indicators I_{as}, I_{afs}, I_{ah}.

Solution	Cost (x10^6€)	I_r	C_u	I_{as}	I_{afs}	I_{ah}
S1	12.7	0.92	0.38	0.92	1.00	1.22
S2	12.5	0.89	0.42	0.94	1.00	1.16
S3	12.7	0.67	0.79	0.98	1.00	1.04
S4	12.8	0.69	0.82	0.99	0.99	1.04

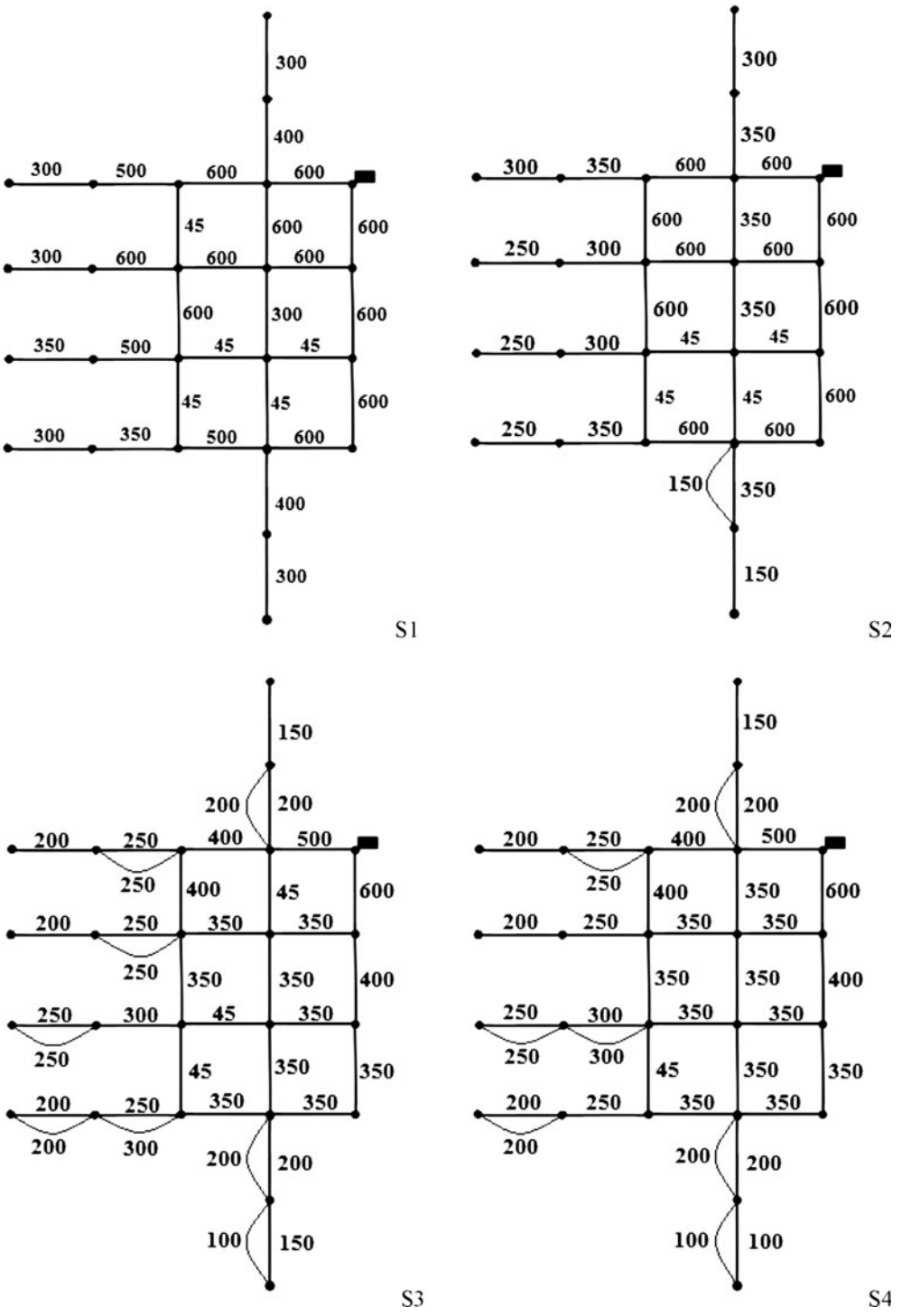

Figure 6. Distribution of diameters (in mm) in the network for solutions S1–S4 of optimization set B.

advantage of encouraging the formation of new loops in correspondence to the branched structures of the network (as is shown in optimization set B), by a) avoiding the coupling of large diameters with small diameters (in order to increase the segments-related reliability) and b) without necessarily entailing the fact that new loops are made up of large diameter pipes alone. This does not come out from the use of the modified resilience index formulated by Prasad et al. (2003) since it refers to the homogeneity of the pipe diameters at nodal level and thus it does not relate to the concept of loop and does not facilitate the formation of new loops.

Conclusions

This work introduces the concept of a loop uniformity index as a potential alternative objective to be compromised with cost and the resilience index, in order to improve the reliable design of water distribution networks. The use of a methodology based on the network multi-objective optimization and on the retrospective evaluation of the optimal solutions in terms of performance indicators has shown that adopting the resilience and the diameter uniformity as two separate objective functions within the optimization process helps to represent network reliability better than the use of the resilience or the modified resilience as single objective functions. In detail, whereas there is no significant difference among the various optimization approaches with reference to the reliability under fire conditions, the advantage of the approach with two reliability related, but different, objectives becomes evident when the network reliability related to the isolation of segments is considered. In the latter case, the new approach makes it possible to obtain solutions which guarantee better service to the users than those obtained on equal cost by considering the resilience (or the modified resilience) alone as a reliability related objective function. Furthermore, when the option of inserting pipes in parallel to the basic pipes in correspondence to the network branched structures is considered within the optimization process, the three-objective optimization approach has the advantage of encouraging the formation of new loops even at low cost conditions, which has a significant impact on the segment isolation related reliability.

It has to be noted that the analysis made in this paper concerned reliability assessment through snapshot simulations, which do not consider the extended period operation of the network. In the latter framework, other reliability aspects (such as the number or the volume of network tanks feeding the network) than those considered herein could also play an important role and would then deserve to be considered.

References

Alvisi, S. and Franchini, M., 2006. Near optimal rehabilitation scheduling of water distribution systems based on a multi-objective genetic algorithm. *Civil Engineering and Environmental Systems*, 23 (3), 143–160.

Alvisi, S., Creaco, E., and Franchini, M., 2011. Segment identification in water distribution systems. *Urban Water Journal*, 8 (4), 203–217.

Aoki, Y., 1998. Flow analysis considering pressure. *In*: *Proceedings of the 49th National Meeting on Waterworks*. Tokyo: Japan Water Work Association, 262–263.

Basupi, I. and Kapelan, Z., 2013. Flexible water distribution system design under future demand uncertainty. *Journal of Water Resources Planning and Management*. doi:10.1061/(ASCE)WR.1943-5452.0000416, published online on October 11, 2013.

Ciaponi, C., 2009. Performance analysis in water supply. *In*: C. Ciaponi, ed. *Performance indicators for the planning, design and management of water supply systems*. Milano: CSDU, 1–29.

Creaco, E., Fortunato, A., Franchini, M., and Mazzola, R., 2014. Comparison between entropy and resilience as indirect measures of reliability in the framework of water distribution network design. *Procedia Engineering*, 70, 379–388. doi:10.1016/j.proeng.2014.02.043.

Creaco, E. and Franchini, M., 2012. Fast network multi-objective design algorithm combined with an a posteriori procedure for reliability evaluation under various operational scenarios. *Urban Water Journal*, 9 (6), 385–399.

Creaco, E. and Franchini, M., 2014a. Low level hybrid procedure for the multi-objective design of water distribution networks. *Procedia Engineering*, 70, 369–378. doi:10.1016/j.proeng.2014.02.042.

Creaco, E. and Franchini, M., 2014b. Comparison of Newton-Raphson global and loop algorithms for water distribution network resolution. *Journal of Hydraulic Engineering* (ISI), 140 (3), 313–321.

Creaco, E., Franchini, M., and Alvisi, S., 2010. Optimal placement of isolation valves in water distribution systems based on valve cost and weighted average demand shortfall. *Water Resources Management*, 24 (15), 4317–4338.

Creaco, E., Franchini, M., and Walski, T.M., 2014a. Accounting for phasing of construction within the design of water distribution networks. *Journal of Water Resources Planning and Management*, 140 (5), 598–606.

Creaco, E., Franchini, M., and Walski, T.M., 2014b. Taking Account of Uncertainty in Demand Growth When Phasing the Construction of a Water Distribution Network. *Journal of Water Resources Planning and Management*. doi:10.1061/(ASCE)WR.1943-5452.0000441, published online on February 8, 2014.

Deb, K., Pratap, A., Agarwal, S., and Meyarivan, T., 2002. A fast and elitist multiobjective genetic algorithm NSGA-II. *IEEE Transactions on Evolutionary Computation*, 6 (2), 182–197.

Farmani, R., Savic, D.A., and Walters, G.A., 2003. Multi-objective optimization of water system: A comparative study. *In*: E. Cabrera, E. Cabrera Jr., ed. *Pumps, Electromechanical Devices and Systems Applied to Urban Water Management*. Lisse: A.A. Balkema, 247–256.

Farmani, R., Walters, G.A., and Savic, D.A., 2005. Trade-Off between Total Cost and Reliability for Anytown Water Distribution Network. *Journal of Water Resources Planning and Management*, 131 (3), 161–171.

Farmani, R., Walters, G., and Savic, D.A., 2006. Evolutionary multi-objective optimization of the design and operation of water distribution network: total cost vs. Reliability vs. Water quality. *Journal of Hydroinformatics*, 8 (3), 165–179.

Gargano, R. and Pianese, D., 2000. Reliability as tool for hydraulic network planning. *Journal of Hydraulic Engineering*, 126 (5), 354–364.

Gessler, J. and Walski, T.M., 1985. *Water distribution system optimization*. Technical Report TREL-85-11. Vicksburg, MS: US Army Corps of Engineers' Waterways Experimentation Station.

Greco, R., Di Nardo, A., and Santonastaso, G., 2012. Resilience and entropy as indices of robustness of water distribution networks. *Journal of Hydroinformatics*, 14 (3), 761–771.

Hashimoto, T., Loucks, D.P., and Stedinger, J., 1982. Reliability, resiliency, and vulnerability criteria for water resource system performance evaluation. *Water Resources Research*, 18 (1), 14–20.

Mays, L.W., 1996. Review of reliability analysis of water distribution systems. *In*: Goulter Tikle, Xu Wasimi, Bouchart, ed. *Stochastic hydraulics '96*. Rotterdam: Balkema, 53–62.

Pandit, A. and Crittenden, J.C., 2012. Index of network resilience (INR) for urban water distribution systems. *Proceedings of the 2012 Critical Infrastructure Symposium*. Retrieved from http://www.tisp.org/index.cfm?cdid=12519&pid=10261

Prasad, T.D. and Park, N.-S., 2004. Multiobjective genetic algorithms for design of water distribution networks. *Journal of Water Resources Planning and Management*, 130 (1), 73–82.

Prasad, T.D., Sung-Hoon, H., and Namsik, P., 2003. Reliability based design of water distribution networks using multi-objective genetic algorithms. *KSCE Journal of Civil Engineering*, 7 (3), 351–361.

Raad, D.N., Sinske, A.N., and van Vuuren, J.H., 2010a. Comparison of four reliability surrogate measures for water distribution systems design. *Water Resources Research*, 46 (5), W05524.

Raad, D.N., Sinske, A.N., and van Vuuren, J.H., 2010b. Multiobjective optimization for water distribution system design using a hyperheuristic. *Journal of Water Resources Planning and Management*, 136 (5), 592–596.

Tanyimboh, T.T. and Templeman, A.B., 2000. A quantified assessment of the relationship between the reliability and entropy of water distribution systems. *Engineering Optimization*, 33 (2), 179–199.

Tanyimboh, T.T., Tabesh, M., and Burrows, R., 2001. Appraisal of source head methods for calculating reliability of water distribution network. *Journal of Water Resources Planning and Management*, 127 (4), 206–213.

Tanyimboh, T.T., Tietavainen, M.T., and Saleh, S., 2011. Reliability assessment of water distribution systems with statistical entropy and other surrogate measures. *Water Science & Technology: Water Supply*, 11 (4), 437–443.

Todini, E., 2000. Looped water distribution networks design using a resilience index based heuristic approach. *Urban Water Journal*, 2 (3), 115–122.

Todini, E. and Pilati, S., 1988. A gradient algorithm for the analysis of pipe networks. *In*: B. Coulbeck and O. Choun-Hou, eds. *Computer application in water supply, volume I – system analysis and simulation*. London: John Wiley & Sons, 1–20.

Walski, T.M., Weiler, J.S., and Culver, T., 2006. Using criticality analysis to identigy impact of valve location. *In*: *Proceedings of 8th Annual Water Distribution Systems Analysis Symposium*, Cincinnati, Ohio, 27–30 August 2006.

Walski, T.M., Chase, D.V., Savic, D.A., Grayman, W., Beckwith, S., and Koelle, E., 2003. *Advanced water distribution modeling and management*. Waterbury, CT: Haestad Press.

Wagner, J.M., Shamir, U., and Marks, D.H., 1988. Water distribution reliability: simulation methods. *Journal of Water Resources Planning and Management*, 114 (3), 276–294.

Wang, Q., Savic, D.A., and Kapelan, Z., 2014. Hybrid metaheuristics for multi-objective design of water distribution systems. *Journal of Hydroinformatics*, 16 (1), 165–177.

Appendix

The main modification made in the NSGA-II algorithm concerned the crowding distance, which represents the distance of the generic individual from its closest neighbors in terms of objective functions. It is a parameter used along with the ranking (i.e. the belonging front) in order to characterize the population individuals. In particular, this parameter is used twice inside the algorithm in order to sort the individuals: the first time when the parents' population has to be built, the second time after the old population is mixed with the offspring population.

The use of the original approach proposed by Deb et al. (2002) for assessing the crowding distance, based on the sorting of the individuals on the basis of the various objective functions, proves reliable in the case of optimization problems with two objective functions (optimizations I and II of the present work). The use of the NSGA-II with the traditional crowding distance for set A optimization III (with three objective functions: cost, I_r, C_u) produces the final Pareto front in Figure 7a, which has two drawbacks: 1 - the dots are not well distributed; 2 – it does not comprise solutions close to the Pareto front obtained with the two objective optimization (cost, I_r); the solutions from the two objective optimization (cost, I_r) are in fact not dominated also when viewed in the context of the three objective functions (cost, I_r, C_u); then part of these solutions should, theoretically, be present in the final Pareto surface.

In order to solve the latter drawbacks, some expedients have to be considered. First of all, a different procedure for assessing the crowding distance in each population front can be used. For a certain individual i, this procedure is based on calculating the Euclidean dimensionless distance from the other generic individual j of the front by applying the following formula:

$$d_{ij} = \sqrt{\left(\frac{f_{1,i} - f_{1,j}}{f_{1,max} - f_{1,min}}\right)^2 + \left(\frac{f_{2,i} - f_{2,j}}{f_{2,max} - f_{2,min}}\right)^2 + \left(\frac{f_{3,i} - f_{3,j}}{f_{3,max} - f_{3,min}}\right)^2}, \tag{12}$$

where $f_{k,i}$ e $f_{k,j}$ are the values of the k-th objective function (with k ranging from 1 to 3) for individuals i and j whereas $f_{k,max}$ and $f_{k,min}$ are the maximum and minimum observed values of the k-th objective function in the front.

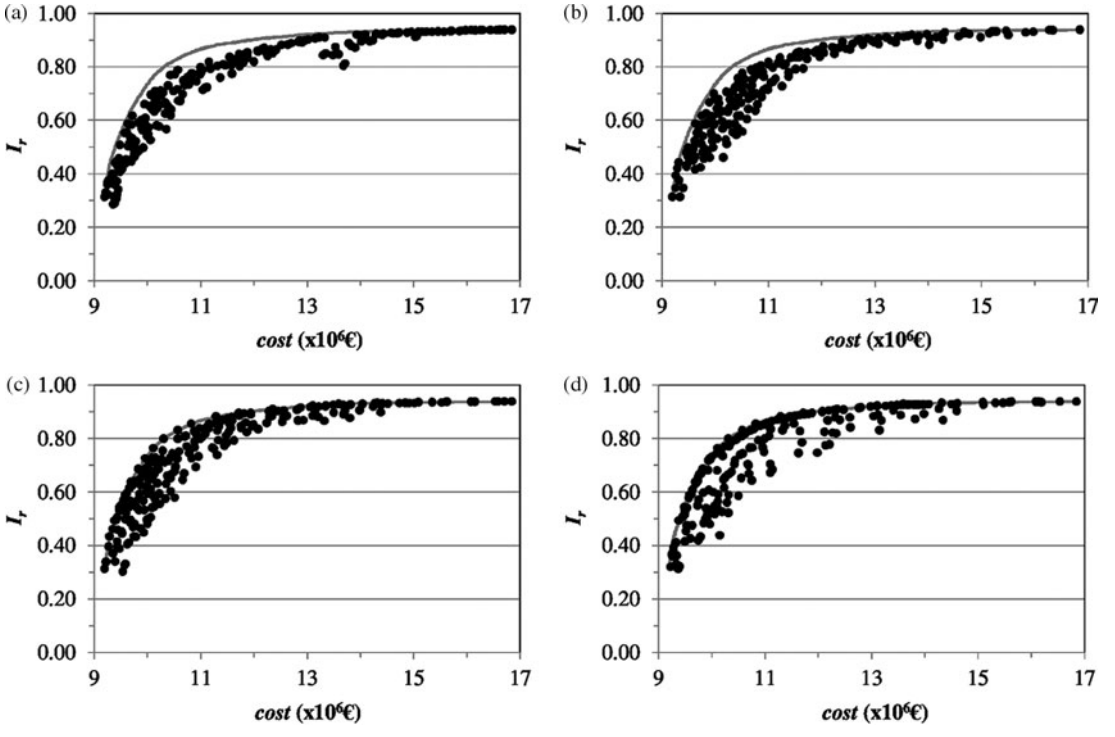

Figure 7. Applications relative to the contents of the Appendix. In all the graphs, dots come from a three objective optimization in the cost-resilience-loop uniformity space whereas the grey line comes from a two objective optimization in the cost-resilience space. Pareto front obtained considering the original crowding distance formula (a); Pareto front obtained considering the new crowding distance formula (b); Pareto front obtained considering the new crowding distance formula and a distance correction coefficient $\xi = 2$ (c); Pareto front obtained considering the new crowding distance formula and a distance correction coefficient $\xi = 5$ (d).

Among all the individuals, the set of neighbors of individual i has then to be built. To this end, for objective function 1, we take those individuals which feature a value of $f_{1,j} > f_{1,i}$; among these individuals, we consider that with the smallest value of d_{ij} as the first member of the set. Subsequently, we take those individuals which feature a value of $f_{1,j} < f_{1,i}$; among these individuals, we consider that with the smallest value of d_{ij} as the second member of the set. By repeating this sequence of instructions for the other objective functions, we complete the set of neighbors for individual i. In the end, the crowding distance d_i of individual i is obtained by averaging the distances of all the neighbors.

By using the procedure above for assessing the crowding distance, we obtain the Pareto front in Figure 7b, which is much better in terms of dot distribution than that in Figure 7a and also presents more dots close to the 2D Pareto front within the cost-resilience space. In order to further improve the latter aspect, the following artifice can be used. Before performing the ranking and calculating the crowding distance for all the individuals on the basis of the three objective functions, it turns out to be convenient to find the non dominated solutions within the subspace made up of the first objective function and the second objective function and within the subspace made up of the first objective function and the third objective function. Once these non dominated individuals in the subspaces have been detected, the ranking can be performed and the crowding distance d_i can be assessed on the basis of the three objective functions. For the subspace non dominated individuals, the value of d_i can be corrected as $d_i = \xi \times d_i$, with $\xi > 1$. By adopting this expedient and considering $\xi = 2$, the Pareto front obtained has some dots close to the two objective Pareto front (see Figure 7c). The only problems of this approach lie in the fact that it:

- slightly increases the number of calculations, and subsequently the computation time;
- needs a 2D Pareto front as a term of comparison;
- requires a certain calibration of parameter ξ. As a matter of fact, a too low value of ξ could vanish the effects, thus leading to the same results as in Figure 7b. On the other hand, a too high value of ξ could make the results of a 3D optimization too similar to those of a 2D optimization (Figure 7d reports the results obtained considering $\xi = 5$, where too many solutions of the 2D optimization are present. i.e. the projection of the Pareto surface tends to collapse onto the 2D front).

However, all the three previous problems are less expensive from the computational viewpoint than the increase in the population and generation size within the optimization process which is the standard action when the optimization problem moves from two to three objective functions.